

Electric dipole moment of the neutron from a flavor changing Higgs-boson

Jan O. Eeg*

*Department of Physics, University of Oslo,
P.O.Box 1048 Blindern, N-0316 Oslo, Norway*

I consider neutron electric dipole moment contributions induced by flavor changing Standard Model Higgs boson couplings to quarks. Such couplings might stem from non-renormalizable $SU(2)_L \times U(1)_Y$ invariant Lagrange terms of dimension six, containing a product of three Higgs doublets. Previously one loop diagrams with such couplings were considered in order to constrain quadratic expressions of Higgs flavor changing couplings to quarks. In the present paper the analysis is extended to the two loop level, where it is possible to generate diagrams for electric dipole moments of quarks with a flavor changing Higgs coupling to *first order only*. Divergent loops are parametrized in terms of an ultraviolet cut-off Λ .

Using the current experimental bound on the neutron electric dipole moment, constraints on Higgs flavor changing couplings are found. From two loop diagrams, and for cut-offs of order one to three TeV, I find a bound of order 10^{-4} for the ($d \rightarrow b$)-type flavor changing Higgs coupling, a bit more relaxed than found previously by other authors from $B_d - \bar{B}_d$ -mixing.

Keywords: CP-violation, Electric dipole moment, Flavor changing Higgs.

PACS: 12.15. Lk. , 12.60. Fr.

I. INTRODUCTION

An electric dipole moment (EDM) for elementary particles is a CP-violating quantity and it gives important information on the matter anti-matter asymmetry in the universe. EDMs of elementary fermions within the Standard Model (SM) are induced through the Cabibbo-Kobayashi-Maskawa (CKM) CP-violating phase. EDMs are studied also within many models

*Electronic address: j.o.eeg@fys.uio.no

Beyond the SM (BSM). For reviews on SM and BSM EDMs, see[1–5]. Experimentally only bounds on electron, muon, proton and neutron EDMs are determined [6]. Explicitly, for the EDM of the neutron (nEDM $\equiv d_n$) discussed in this paper, the present experimental bound is [7]

$$d_n^{exp}/e \leq 2.9 \times 10^{-26} \text{ cm} . \quad (1)$$

Within the SM, the nEDM is calculated to be several orders of magnitudes below the experimental bound. Calculations of the nEDM will in general put bounds on hypothetical models BSM, and any measured nEDM significantly bigger than the SM estimate (10^{-32} to $10^{-31} e \text{ cm}$) would signal New Physics.

The SM contributions to the nEDM are well known and thoroughly explained in [1]. At a low energy scale one can construct an effective Lagrangian

$$\mathcal{L}_{\text{eff}} = \mathcal{L}_4 + \mathcal{L}_5 + \mathcal{L}_6 + \dots , \quad (2)$$

with all possible CP-odd operators of appropriate dimension. The QCD-odd term gives the dimension 4 operator [1, 5]. The dimension 5 operator contains electric dipole moment operators as well as color electric operators of quarks. The CP-odd three-gluon Weinberg operator and four-fermion interactions are then in the class of dimension six operators [1–3], which are not subject of this study. The electric dipole moment of a single fermion in (2) has the form

$$\mathcal{L}_{5,\text{em}} = \frac{i}{2} d_f \bar{\psi}_f \sigma_{\mu\nu} F^{\mu\nu} \gamma_5 \psi_f , \quad (3)$$

where d_f is the electric dipole moment of the fermion, ψ_f is the fermion (quark) field, $F^{\mu\nu}$ is the electromagnetic field tensor, and $\sigma_{\mu\nu} = i[\gamma_\mu, \gamma_\nu]/2$ is the dipole operator in Dirac space. The electric dipole operator in (3) for quarks appears within the SM from three loop diagrams with double Glashow-Iliopoulos-Maiani (GIM)- cancellations and in addition a gluon exchange. These are of order $\alpha_s G_F^2$, and are proportional to quark masses and an imaginary CKM factor. They were found to be very small, of order $10^{-34} e \text{ cm}$ [8, 9]. Still within the SM, many contributions to the nEDM due to interplay of quarks in the neutron, were studied [1, 10–19]. These mechanisms, gave results of order 10^{-33} to $10^{-31} e \text{ cm}$.

The nEDM due to EDMs of light u - and d -, and even s -quarks are given by the formula

$$d_n = \gamma_u d_u + \gamma_d d_d + \gamma_s d_s , \quad (4)$$

similar to a corresponding formula for the magnetic moment. In the strict valence approximation,

$$\gamma_u = -\frac{1}{3}, \quad \gamma_d = \frac{4}{3}, \quad \gamma_s = 0, \quad (5)$$

while recent lattice calculations [20, 21] give

$$\gamma_u = -0.22 \pm 0.03, \quad \gamma_d = 0.74 \pm 0.07, \quad \gamma_s = 0.008 \pm 0.010. \quad (6)$$

Note that there is a contribution to the nEDM from the EDM of the s -quark, with a small coefficient.

Many models BSM suggest possible new particles or new interactions inducing EDMs [1–5, 10, 22–32]. In the case of New Physics presence, flavor physics might be testable through CP-violating asymmetries in mesonic decays [23, 24, 33]. The properties and couplings of the physical Higgs boson (H) are still not completely known. Some authors [34–39] have suggested that the physical Higgs boson might have flavor changing couplings to fermions which might also be CP-violating. In these papers bounds on quadratic expressions of such couplings were obtained from various processes, say, like $K - \bar{K}$, $D - \bar{D}$, and $B - \bar{B}$ - mixings, and also from leptonic flavor changing decays like $\mu \rightarrow e\gamma$ and $\tau \rightarrow \mu\gamma$. In the latter case two loop diagrams of Barr-Zee type [40] were also considered [34–36, 41]. (See also [42]). Flavor changing couplings of this type will occur if the SM Higgs have non-renormalized interactions appearing when higher mass states are integrated out. For instance, flavor changing Higgs (FCH) couplings might stem from $SU(2)_L \times U(1)_Y$ -invariant but non-renormalizable Lagrangian terms of dimension six.

In this paper I extend the analysis of [35, 36] to two loop diagrams. Some of these give contributions suppressed by the small mass ratio m_d/M_W for the ordinary SM Higgs coupling to fermions. (M_W denotes the mass of the W -boson and m_q is the mass of the quark q). However, if the Higgs is coupled to a top (t) quark one might obtain relevant non-suppressed contributions. Motivated by the result of the previous work [32], I consider such diagrams. There are additional reasons to extend the analysis in [35, 36] for nEDM to two loop level. Namely, it will be demonstrated that one might obtain amplitudes with the unknown couplings to first order only. Also, in general, it is known that some two loop diagrams might give bigger amplitudes than one loop diagrams because of helicity flip(s) in the latter [35, 36, 41, 43]. In the present case, two loop amplitudes will be proportional to a large ttH coupling or a large WWH coupling within the SM, in contrast to the small SM

Higgs couplings to light fermions. This might compensate for the two loop suppression of the diagrams.

In the next section (II) I will present the framework for the FCH couplings. In the sections III and IV two loop calculations for the FCH couplings will be presented. In section V the results will be discussed, and the conclusion given.

II. FLAVOR CHANGING PHYSICAL HIGGS?

Within the framework in [34–39] (see also ref. [44]) the effective interaction Lagrangian for the FC transition $f_1 \rightarrow f_2$ due to Higgs exchange can in general be written

$$\mathcal{L}_{\text{eff}} = Y_R(f_1 \rightarrow f_2) \cdot \overline{(f_2)_L} H (f_1)_R + Y_L(f_1 \rightarrow f_2) \cdot \overline{(f_2)_R} H (f_1)_L + h.c. , \quad (7)$$

where $f_{1,2}$ are fermion fields, H the Higgs field and $Y_{L,R}(f_1 \rightarrow f_2)$ are coupling constants. The Y 's are in general thought to be complex numbers. Then, from the hermitean conjugation part we obtain for the opposite $f_2 \rightarrow f_1$ transition

$$Y_L(f_2 \rightarrow f_1) = Y_R(f_1 \rightarrow f_2)^* \quad \text{and} \quad Y_R(f_2 \rightarrow f_1) = Y_L(f_1 \rightarrow f_2)^* . \quad (8)$$

Flavor changing Higgs couplings of the type presentes in eq. (7) may occur if there are non-renormalizable Higgs type Yukawa-like interactions due to dimension six operators, as shown explicitly in [36, 39] :

$$\mathcal{L}^{(D)} = -\lambda_{ij} \overline{Q}_i \phi D_j - \frac{\tilde{\lambda}_{ij}}{\Lambda_{NP}^2} \overline{Q}_i \phi D_j (\phi)^\dagger \phi + h.c. , \quad (9)$$

where the generation indices i and j are understood to be summed over. Further, ϕ is the SM Higgs field, Q_i is the left-handed $SU(2)_L$ quark doublets, and the D_j 's are the right-handed $SU(2)_L$ singlet d -type quarks in a general basis. Further, Λ_{NP} is the scale where New Physics is assumed to appear. There is a similar term as in (9) for right-handed type u -quarks, U_j .

Using the assumptions based on (7), one obtains one loop diagrams for EDMs of u - and d -quarks [35, 36]. The one loop diagram in Fig. 1 - with FCH coupling at both vertices, puts bounds on *quadratic* expressions of the Y 's for definite choices of flavor. Note that this diagram gives a finite contribution to quark EDMs.

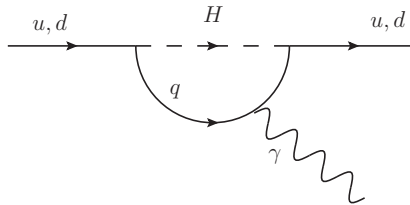


FIG. 1: One loop diagrams for EDMs of u - and d -quarks with FC Higgs couplings. Here $q = s, b$ for an EDM of the d -quark and $q = c, t$ for an EDM of a u -quark.

III. DIAGRAMS WITH ONE FC COUPLING -AND A $t\bar{t}H$ -COUPLING

In Fig. 2 is shown two loop diagrams for the EDM of a d -quark generated by exchange of one physical Higgs (H) boson and one W -boson, with a sizeable Higgs coupling $\sim g_W m_t/M_W$ to a top quark and where only *one* of the Higgs couplings are flavor changing (a soft photon is assumed to be added). The non-crossed version to the left in Fig. 2 does not give non-suppressed contributions. Taking crossed Higgs and W -bosons are equivalent to the topologies in the middle and right of Fig. 2.

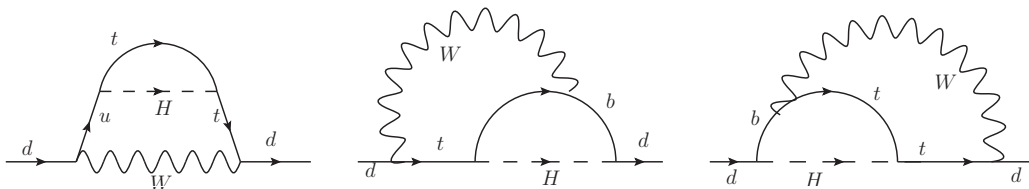


FIG. 2: Three diagrams with FC Higgs coupling for EDMs of a d -quark. Soft photon emission from one of the charged particles is assumed to be added. The left diagram will give contributions suppressed by $m_{u,d}/M_W$. Taking the crossed diagrams in the center or to the right, we will get contributions which are not suppressed by light quark masses. The diagram to the right is the complex conjugate of the diagram in the center.

Adding a soft photon to the diagram in the middle and to the right, we get four diagrams for both cases. In Fig. 3 the four diagrams obtained by adding a soft photon emission to

the diagram to the right in Fig. 2 are shown.

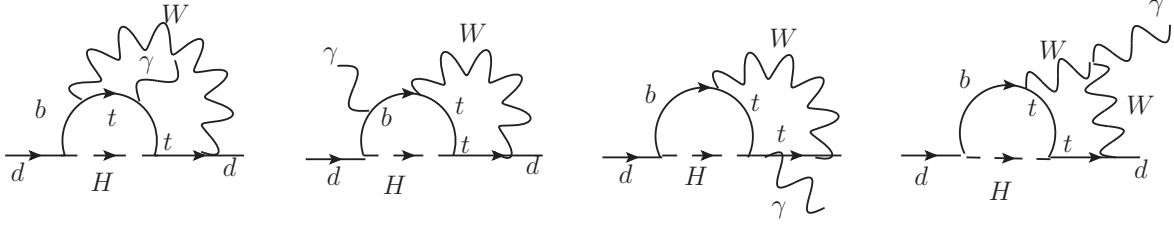


FIG. 3: Four diagrams for an EDM of a d quark obtained by adding a soft photon to the diagram to the right of Fig. 2. For the first three diagrams, there are also corresponding diagrams where the W -boson is replaced by an unphysical Higgs-boson within Feynman gauge.

The results for the loop contributions in Fig. 3 have the form:

$$\mathcal{M}(f \rightarrow f\gamma)_{(a)} = A (\bar{f} \sigma \cdot F P_R f) , \quad (10)$$

and the diagrams with interchanged order of H and W loops, as in the middle of Fig. 2 have the form:

$$\mathcal{M}(f \rightarrow f\gamma)_{(c)} = A^* (\bar{f} \sigma \cdot F P_L f) , \quad (11)$$

where $P_L = (1 - \gamma_5)/2$ and $P_R = (1 + \gamma_5)/2$ are projectors in Dirac space. Then the electric dipole moment is found to be:

$$(d_f)_{2-loop} = 2 \text{Im}(A). \quad (12)$$

There is also a contribution to the magnetic moment (i.e the gyromagnetic quantity $(g - 2)$) given by $2 \text{Re}(A)$.

The contributions from the four diagrams ($i = 1-4$) in Fig. 3 and its complex conjugates can then, by using (12) be written

$$\left(\frac{d_d}{e}\right)_i = \hat{e}_i F_2 S_i \text{Im}[Y_R(d \rightarrow b) V_{td}^* V_{tb}] \quad (13)$$

where the \hat{e}_i 's are the electric charges (in units $e =$ the proton charge) of the photon-emitting particles, i.e. $\hat{e}_{1,3} = \hat{e}_t = +2/3$, $\hat{e}_2 = \hat{e}_b = -1/3$, and $\hat{e}_4 = \hat{e}_W = +1$. Here I have used the

relations (8) and (12). The V 's are CKM matrix elements in the standard notation. The constant F_2 sets the overall scale of the EDMs obtained from our two loop diagrams:

$$F_2 = \frac{g_W^3}{M_W \sqrt{2}} \left(\frac{1}{16\pi^2} \right)^2 = \frac{2M_W^2}{v^3} \left(\frac{1}{16\pi^2} \right)^2 \simeq 6.94 \times 10^{-22} \text{ cm} , \quad (14)$$

where I have used the conversion rule $1/(200\text{MeV}) = 10^{-13}\text{cm}$. The quantities S_i in (13) are dimensionless and given by integrals over one Feynman parameter. Details from the loop calculations are given in the Appendix. For the first two diagrams, given in the formulae (48)-(50), the loop functions S_1 and S_2 are finite and depend on the mass ratios

$$u_t = (m_t/M_W)^2 = 4.64 \quad , \quad u_H = (M_H/M_W)^2 = 2.44 . \quad (15)$$

Numerically, I find

$$S_1 = -2.55 \quad ; \quad S_2 = 2.50 . \quad (16)$$

If the soft photon is emitted from the top quark after exchange of the Higgs boson, as in the third diagram from left in Fig. 3, or from the W -boson in the fourth diagram, the left sub-loop containing the Higgs boson is logarithmically divergent, which is not unexpected because the interaction in (9) is non-renormalizable.

Using Feynman gauge for the W -boson, one has also to add diagrams with the unphysical Higgs ϕ_{\pm} (*i.e.* the longitudinal component of the W -boson) given by the the Lagrangian

$$\mathcal{L}_{\phi\text{td}} = -\frac{g_W}{M_W} V_{td}^* \bar{d} \phi_{-} (m_d P_L - m_t P_R) t + h.c. . \quad (17)$$

The total contribution from the third diagram in Fig. 3 (including the contribution from the unphysical Higgs), is

$$S_3 = u_t p_1(u_t) C_{\Lambda} + 1.81 . \quad (18)$$

Here the UV divergence is parametrized through the quantity

$$C_{\Lambda} \equiv \ln\left(\frac{\Lambda^2}{M_W^2}\right) + \frac{1}{2} , \quad (19)$$

where Λ is the UV cut-off. Numerically, C_{Λ} is ~ 5.5 to ~ 7.7 for $\Lambda \sim 1$ to 3 TeV. Further,

$$p_1(u) \equiv \frac{u}{(u-1)} \left(1 - \frac{\ln(u)}{u-1} \right) \quad ; \quad p_1(u_t) = 0.737 , \quad (20)$$

where u_t is given in (15).

The fourth diagram in Fig. 3 with the soft photon emitted from the W -boson again contains a divergent part, and the total contribution to the fourth diagram is

$$S_4 = -\frac{3}{4} p_2(u_t) C_\Lambda + 2.98 , \quad (21)$$

where

$$p_2(u) \equiv \frac{u}{(u-1)} \left(\frac{u \cdot \ln(u)}{u-1} - 1 \right) ; \quad p_2(u_t) = 1.219 . \quad (22)$$

Summing all contributions from diagrams in Fig. 3, we find

$$\left(\frac{d_d}{e}\right)_{Fig.3} = (1.65 + 1.37 C_\Lambda) \cdot F_2 \cdot Im[Y_R(d \rightarrow b) V_{td}^* V_{tb}] . \quad (23)$$

There are in addition contributions from the same diagrams in Fig. 3, but with other quarks in the loop. If the b -quark is replaced by an s -quark, the CKM factors are two orders of magnitude smaller, and in addition $Y_R(d \rightarrow s)$ has a stricter bound from $K - \bar{K}$ -mixing. If the t -quark is replaced by the u - or c -quark, the contributions are suppressed by $(m_u/m_t)^2$ and $(m_c/m_t)^2$, respectively.

There are also similar diagrams for EDM of an u -quark, *i.e.* like in Fig. 3 with the t - and the b -quarks interchanged. This amplitude has the same structure as in (13), and is proportional to the combination $Im[Y_R(u \rightarrow t) \cdot V_{tb}^* V_{ub}]$. But the u -quark EDM contributions will be neglected. First, the ordinary SM coupling of the Higgs will be proportional to m_b/M_W instead of m_t/M_W for the d -quark case. Then it turns out that the prefactors S_i for u -quark EDM contributions are suppressed by a factor of order $(m_b/m_t)^2 \sim 10^{-3}$ compared to the analogous d -quark contributions. Second, the absolute value of $Y_R(u \rightarrow t)$ has a relaxed bound of order one, but because it comes from a similar lagrangian term as in (9) one might guess that it is of same order of magnitude as $Y_R(b \rightarrow b)$. And, moreover, even if the ratio between $Y_R(u \rightarrow t)$ and $Y_R(b \rightarrow b)$ would be of order m_t/m_b , the u -quark EDM contribution to the nEDM in (4) would still be suppressed by $(\gamma_u \cdot m_b)/\gamma_d \cdot m_t \sim 10^{-2}$ compared to the d -quark EDM contribution to the nEDM.

IV. DIAGRAMS WITH ONE FC COUPLING -AND A WWH -COUPLING

We will now consider another class of two loop diagrams generated by FC Higgs-boson couplings. These diagrams shown in Fig. 4 have a big WWH -coupling $\sim g_W M_W$ and *only one* FC Higgs coupling to a fermion. These two loop diagrams are divided in three types: the

(a)-diagrams with Higgs exchange to the left, the (b)-diagrams with Higgs exchange in the middle, and the (c)-diagrams with Higgs exchange to the right. In the limit of zero external light quark momenta, which we work, the (b)-diagrams are zero due to (odd) momentum integration, or they are suppressed by small external quark masses. The (c)-diagrams are complex conjugates of the (a)-diagrams. Soft photon emission from one of the charged particles should of course be added in Fig. 4, as seen in Fig. 5 for the (a)-diagrams. The (a) diagrams give contributions like in (10), and the (c) diagrams like in (11).

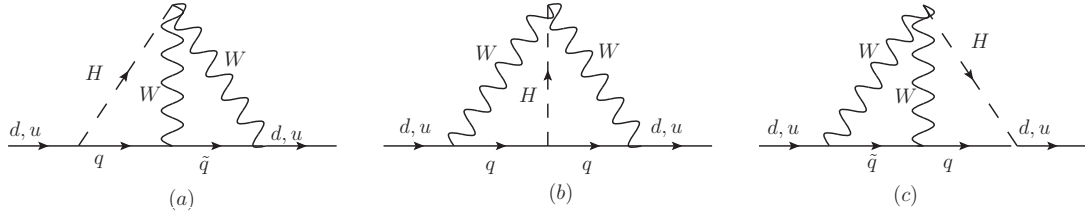


FIG. 4: Three diagrams with one WWH -Higgs coupling and one FC Higgs coupling for EDMs of a u - or d -quark. Soft photon emission from one of the charged particles is assumed to be added. The (b) diagrams are zero in the limit of zero external momentum of the light quarks due to momentum integration, or are suppressed by small light quark masses. The (c) diagrams are complex conjugates of the (a) diagrams. Here $q = s, b$ and $\tilde{q} = u, c, t$ for EDM of a d -quark, and $q = c, t$ and $\tilde{q} = d, s, b$ for EDM of a u -quark.

The relevant piece of the SM Lagrangian for a Higgs coupling to two W -bosons is given by

$$\mathcal{L}_{\text{WWH}} = g_W M_W \sqrt{2} H W^{(-)\mu} W_\mu^{(+)} . \quad (24)$$

Using Feynman gauge for the W -boson, we must also consider Lagrangian terms for a physical Higgs coupling to a W -boson and the unphysical Higgs boson ϕ_\pm . In addition to the term for quarks coupling to ϕ_\pm in (17), there is the relevant $HW\phi_\pm$ - coupling obtained from the Lagrangian

$$\mathcal{L}_{\text{HW}\phi} = \frac{g_W}{\sqrt{2}} \{ H (i\partial^\mu \phi_-) - (i\partial^\mu H)\phi_- \} W_\mu^{(+)} + h.c. \quad (25)$$

Because of derivative couplings, the vertices involving the unphysical Higgs ϕ_\pm will depend on the loop momenta, which might give divergent (sub-)loops. There are also $W\gamma\phi_\pm$ -couplings, but they do not contribute for soft photon emission.

In the preceding section (III) all numerically relevant diagrams were proportional to m_t^2 , and even m_t^4 in S_3 . In the present section the diagrams have another chiral structure, and we get diagrams $\sim m_t^2$ only for the case when the W -boson is replaced by an unphysical Higgs ϕ_{\pm} . Therefore I apriori consider all quark flavors in the loops, although it is expected that the GIM-mechanism will cancel the leading terms with light quark flavors.

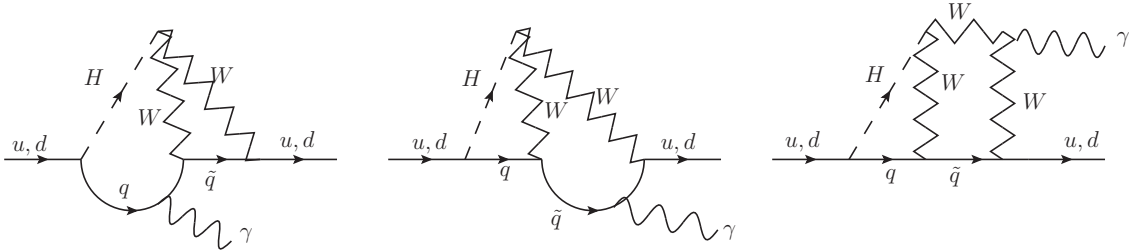


FIG. 5: Emission of a soft photon from (a)-type diagrams of Fig. 4. There is also a diagram with emission from the W in center of the diagram, and in addition graphs with the W replaced by an unphysical Higgs within Feynman gauge.

Contributions to the d -quark EDM from soft photon emission from the quark $q = s, b$ in the diagram 5a, (*i.e.* to the left in Fig. 5) can be written :

$$\begin{aligned} \left(\frac{d_d}{e}\right)_{5a} = & -2 \hat{e}_s F_2 \{ \text{Im} [Y_R(d \rightarrow s) \lambda_u] \cdot \Delta f_d(s, u - c) + \text{Im} [Y_R(d \rightarrow s) \lambda_t] \cdot \Delta f_d(s, t - c) \} \\ & - 2 \hat{e}_b F_2 \{ \text{Im} [Y_R(d \rightarrow b) \xi_u] \cdot \Delta f_d(b, u - c) + \text{Im} [Y_R(d \rightarrow b) \xi_t] \cdot \Delta f_d(b, t - c) \} \end{aligned} \quad (26)$$

where F_2 is given in (14) and where $\hat{e}_s = \hat{e}_b = -1/3$ are charges for the photon-emitting quarks, and the λ 's and the ξ 's are CKM factors:

$$\lambda_{\tilde{q}} = V_{\tilde{q}d}^* V_{\tilde{q}s} , \quad \xi_{\tilde{q}} = V_{\tilde{q}d}^* V_{\tilde{q}b} , \quad \tilde{q} = u, c, t . \quad (27)$$

Note that only the right-handed couplings Y_R contribute to the amplitude, due to the chiral structure of the two loop diagrams. Within the Wolfenstein parametrization, λ_t is of fifth order in $\lambda = \lambda_u$, while ξ_u and ξ_t are only of third order. The Δf 's in (26) are differences, due to GIM-cancellation, between loop functions $f(q, \tilde{q})$, for given flavors $q = s, b$ and $\tilde{q} = u, c, t$.

These are functions of quark, W -boson and Higgs masses and are integrals over *one* Feynman parameter involving logarithmic and dilogarithmic functions, and is given in eq. (65) in the Appendix. Above, we have used the shortages

$$\Delta f_d(b, t - c) \equiv f(b, t) - f(b, c) \quad ; \quad \Delta f_d(s, t - c) \equiv f(s, t) - f(s, c) \quad , \quad (28)$$

and so on in a self-explanatory way.

The quantities $f(q, \tilde{q})$ are finite, and are of order 10^{-1} to 1. (See Table I and II). The GIM-cancellations for the difference between the u - and c -quark contributions are very efficient, such that the differences $\Delta f_d(s, u - c)$ and $\Delta f_d(b, u - c)$ are of order 10^{-3} to 10^{-7} , and can be safely neglected. Contributions with the t -quark in the loops are significantly different from contributions involving the lighter quarks. Thus, the determination of *both* the t -quark *and* the c -quark contributions will be important. In this case the GIM cancellation is not efficient. This pattern is confirmed in the tables I-VI in the Appendix. The differences between the c , and t -contributions are still of order 10^{-1} to 1. Numerically,

$$\Delta f_d(s, t - c) \simeq \Delta f_d(b, t - c) \simeq -0.34 \quad . \quad (29)$$

As the $f_d(q, u - c)$'s are very small, and λ_t is of order λ^5 , while ξ_t is of order λ^3 , we find that the contribution proportional to $\xi_t \cdot \Delta f_d(b, t - c)$ dominates in equation (26). Also, $Y_R(d \rightarrow s)$ has a stricter bound from $K - \bar{K}$ -mixing than $Y_R(d \rightarrow b)$ has from $B_d - \bar{B}_d$ -mixing [36].

Similar to (26), contributions to the u -quark EDM due to emission from the quark $q = c, t$ the diagram to the left in Fig. 5 is :

$$\begin{aligned} \left(\frac{d_u}{e}\right)_{5a} = & -2 \hat{e}_c F_2 \{ \text{Im} [Y_R(u \rightarrow c) \kappa_d] \cdot \Delta f_u(c, d - s) + \text{Im} [Y_R(u \rightarrow c) \kappa_b] \cdot \Delta f_u(c, b - s) \} \\ & - 2 \hat{e}_t F_2 \{ \text{Im} [Y_R(u \rightarrow t) \zeta_d] \cdot \Delta f_u(t, d - s) + \text{Im} [Y_R(u \rightarrow t) \zeta_b] \cdot \Delta f_u(t, b - s) \} \end{aligned} \quad (30)$$

where the κ 's and the ζ 's are CKM factors:

$$\kappa_{\tilde{q}} = V_{u\tilde{q}}(V_{c\tilde{q}})^* \quad , \quad \zeta_{\tilde{q}} = V_{u\tilde{q}}(V_{t\tilde{q}})^* \quad , \quad \tilde{q} = d, s, b \quad . \quad (31)$$

Within the Wolfenstein parametrization, $\kappa_d = -\lambda$, κ_b is of fifth order, while ζ_d and ζ_b are of third order in λ . Further, the Δf_u 's are defined as

$$\Delta f_u(u, b - s) \equiv f(u, b) - f(u, s) \quad ; \quad \Delta f_u(t, b - s) \equiv f(t, b) - f(t, s) \quad , \quad (32)$$

and so on in a self-explanatory way. For the EDMs of the u -quark, the values of the various (Δf_u) 's are of order 10^{-3} to 10^{-7} after GIM-cancellation, and can be neglected, as seen in

table II in the Appendix. Again, we neglect the u -quark EDM, for the same reasons given at the end of the preceding section.

The diagram with soft photon emission from the quark $\tilde{q} = u, c, t$, is shown the center of Fig. 5 (*i.e* Fig. 5b). In this case the loop functions are named $h(q, \tilde{q})$. Adding contributions where the W is replaced by an unphysical Higgs ϕ_{\pm} , we obtain divergent contributions for these loop functions. Because the $WH\phi_{\pm}$ -vertex is momentum dependent, the left subloop is divergent, reflecting again that the theory based on the Lagrangian in eq. (7) alone is not renormalizable.

The contribution(s) from the diagram in Fig. 5b has the same structure as in (26) and (30), but all terms are not numerically relevant. The numerically relevant term from the $h(q, \tilde{q})$ -functions is given by:

$$\left(\frac{d_d}{e}\right)_{5b} \simeq +2 \hat{e}_{\tilde{q}} F_2 \cdot \text{Im} [\xi_t Y_R(d \rightarrow b)] \cdot \Delta h_d(b, t - c) , \quad (33)$$

where $\Delta h_d(b, t - c)$ is defined similar to the Δf 's in eq.(28). From the Appendix one finds

$$\Delta h_d(b, t - c) = p_2(u_t) C_{\Lambda} - 1.26 , \quad (34)$$

where C_{Λ} is given in (19) and $p_2(u)$ in (22).

For diagrams with a soft photon emitted from the W -boson, as shown at the right of Fig. 5 (Fig. 5c), the loop functions are named $k(q, \tilde{q})$. Also in this case there are divergent diagrams, because the left sub-loop might be divergent for the replacement $W \rightarrow \phi_{\pm}$. After GIM-cancellation the dominant term is

$$\left(\frac{d_d}{e}\right)_{5c} \simeq 3 \hat{e}_W F \cdot \text{Im} [Y_R(d \rightarrow b) \xi_t] \cdot \Delta k_d(b, t - c) , \quad (35)$$

where from the Appendix one finds

$$\Delta k_d(b, t - c) = \frac{1}{2} p_2(u_t) C_{\Lambda} - 2.48 \quad (36)$$

Neglecting small contributions (all except those proportional to $V_{td}^* V_{tb} \equiv \xi_t$), and summing all contributions from diagrams in Fig. 5 one finds

$$\left(\frac{d_d}{e}\right)_{Fig.5} = (3.46 C_{\Lambda} - 9.35) \cdot F_2 \cdot \text{Im}[Y_R(d \rightarrow b) V_{td}^* V_{tb}] \quad (37)$$

The EDM of the u -quark is neglected due to small loop functions (-after GIM-cancellation), small CKM-factors. Moreover, the comments about the Y_R 's at the end of the previous sections are also relevant here.

V. SUMMARY AND CONCLUSION

As expected, there are cases where the considered two loop diagrams for the EDMs of d - and u -quarks diverges. This happens for cases in section III where the left sub-loop in Fig. 6 is involved, and for diagrams where the unphysical Higgs (ϕ_{\pm}) is involved both in sect III and IV. More specific, the left diagram in Fig. 6 which looks like a vertex correction for $d \rightarrow W + u, c, t$ is logarithmically divergent. Actually, this diagram generates a logarithmic divergent *right-handed current* which has no match in the SM. The diagram at the right in Fig. 6 is convergent, but if the W -boson is replaced by an unphysical Higgs ϕ_{\pm} , when used in two loop diagrams as in Fig. 5, we obtain logarithmic divergent diagrams due to a momentum dependent vertex, as seen from (25). These are numerically relevant if the quark \tilde{q} is a top quark. The dominating divergent terms in section III and IV are proportional to m_t^2 (-or even m_t^4 in one case in section III). It should also be noted that the first and last diagram in Fig. 5 are relevant for the EDM of the electron [45]. However, in that case the divergent terms would be proportional to powers of a tiny neutrino mass, instead of the top-quark mass.

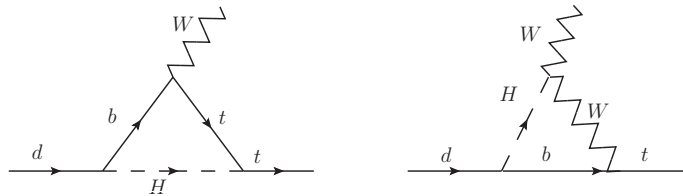


FIG. 6: The divergent effective W-loop vertex correction diagram relevant for diagrams of section III (left), and the (finite) effective vertex correction relevant for diagrams in section IV (right).

Summing all two loop contributions from section III and IV, we obtain the dominating contribution for an EDM of the d -quark:

$$\left(\frac{d_d}{e}\right)_{Tot} = (4.83 C_{\Lambda} - 7.70) F_2 \text{Im}[Y_R(d \rightarrow b) V_{td}^* V_{tb}] . \quad (38)$$

All contributions (after GIM-cancellation) not proportional to $\xi_t \equiv V_{td}^* V_{tb}$ are neglected, using bounds on other Y_R 's [35, 36], as explained in the preceding sections. Also all the

contributions for an EDM of the u -quark can be neglected, for reasons given at the end of the sections III and IV.

I have also neglected the s -quark contribution d_s for the following reason: The loop functions for the s -quark are numerically close to the ones for the d -quark. The CKM factor is bigger, but $\gamma_s/\gamma_d \simeq 10^{-2}$, such that the contribution to the result in (4) from the d_s is of order 5%. Also, because we are dealing with an effective theory with limited precision, we do not consider the mixing of color electric terms into the EDM term in (3) due to renormalization effects in perturbative QCD. Thus our final result for the nEDM is simply

$$d_n \simeq \gamma_d d_d, \quad (39)$$

where the lattice value of γ_d is given in (6). Using the experimental bound for nEDM in (1), the result (38) of the present study gives the bound

$$|\text{Im} \left[Y_R(d \rightarrow b) \cdot \frac{V_{td}^* V_{tb}}{|V_{td}^* V_{tb}|} \right]| \leq (2.0 \text{ to } 3.2) \times 10^{-4}. \quad (40)$$

for values of $\Lambda = 1$ to 3 TeV, where New Physics might be thought to appear. From the mathematical point of view, Λ is the quantity which regularise the divergent two loop diagrams, while Λ_{NP} in (9) is introduced as a dimensional quantity parametrising the Y_R 's and indicates the scale of new physics. But these scales are expected to be of the same order of magnitude.

In (40) I have found a bound on the coupling $Y_R(d \rightarrow b)$ comparable to, but slightly more relaxed than previous bounds [35, 36]. Also, the bound found here is not directly on the absolute value, as in [35, 36], but on a combination of $Y_R(d \rightarrow b)$ and a CKM factor, Turned around, if the bound for $Y_R(d \rightarrow b)$ found in [36] is (almost) saturated, then a value for nEDM not too far below the bound in (1) can not be excluded. This might be illustrated explicitly as follows:

Using (38), the lattice values in (6) and absolute value of $V_{td}^* V_{tb}$ from [6], one may write my result for the nEDM in the following way

$$d_n/e \simeq N_\Lambda \times \left\{ \frac{|Y_R(b \rightarrow d)|}{|Y_R(b \rightarrow d)|_{Bound}} \cdot \text{Im} \left[\frac{Y_R(d \rightarrow b)}{|Y_R(b \rightarrow d)|} \cdot \frac{V_{td}^* V_{tb}}{|V_{td}^* V_{tb}|} \right] \right\} \times 10^{-26} \text{ cm}, \quad (41)$$

where I have scaled the result with the bound from [35, 36]:

$$|Y_R(d \rightarrow b)| \leq 1.5 \times 10^{-4} \equiv |Y_R(d \rightarrow b)|_{Bound}. \quad (42)$$

Explicitly, the function N_Λ , deduced from (38) can be written

$$N_\Lambda = \alpha \cdot (C_\Lambda - \beta) , \quad (43)$$

where $\alpha = 0.31$ and $\beta = 1.59$. This function is plotted as a function of Λ in Fig. 7.

Now, the *maximal value* of the parenthesis $\{\dots\}$ in (41) is $= 1$. Then, *if* the bound for $Y_R(d \rightarrow b)$ is saturated, the plot for the function N_Λ in Fig. 7 shows that when the cut-off Λ is stretched up to 25 TeV, the bound for nEDM in (1) is reached. On the other hand, if the bound for $Y_R(d \rightarrow b)$ is reduced, and also Λ is reduced, my value for nEDM will be accordingly smaller.

I stress that the result (41) depends only on two unknowns, the flavor changing (FC) Higgs coupling $Y_R(d \rightarrow b)$, and the value of the cut-off scale Λ .

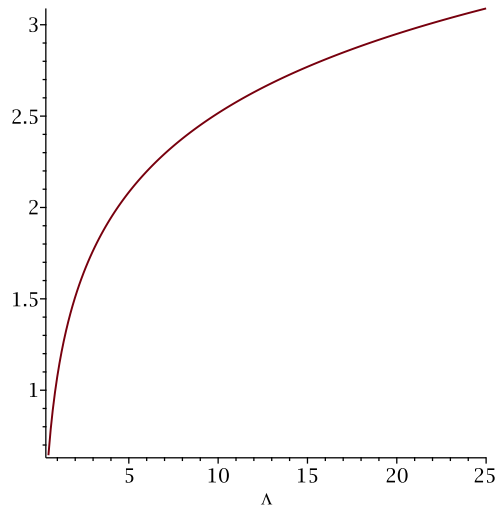


FIG. 7: The quantity N_Λ as a function of cut-off Lambda (in TeV)

In conclusion, I have explored the consequences for the nEDM of having flavor changing Higgs couplings. In the scenario of [36, 39] such couplings might stem from a six dimensional non-renormalizable, $SU(2)_L \times U(1)_Y$ gauge-invariant Lagrangian piece proportional to the third power of the SM Higgs doublet field, as seen in eq. (9). In the present paper the analysis in [35, 36] is extended to two loop case for quark EDMs generated by a flavor changing Higgs coupling Y_R to first order.

I have found and calculated two loop contributions which gives a bound for the imaginary part of $Y_R(d \rightarrow b)$ slightly more relaxed, but of the same order of magnitude compared to the bound found in [35, 36] for the absolute value, obtained from $B_d - \bar{B}_d$ -mixing. Turned around, if the bound for $Y_R(d \rightarrow b)$ found in [35, 36] is almost saturated, a value for nEDM not far below the bound in (1) cannot be excluded.

VI. APPENDIX DETAILS FROM THE TWO OOP CALCULATIONS

To simplify calculations I use the effective quark propagator in a soft electromagnetic field F [46]:

$$S_1(k, F) = \left(-\frac{e_q}{4}\right) \frac{\{(\gamma \cdot k + m_q), \sigma \cdot F\}}{(k^2 - m_q^2)^2}, \quad (44)$$

where k is the four momentum and m_q the mass of the quark q . The notation $\{A, B\} \equiv AB + BA$ is used. Similarly, for emission of a soft photon from a W -boson, the effective propagator is:

$$(D_1(k, F))^{\alpha\beta} = \left(-\frac{e_W}{4}\right) \frac{3i (g^{\mu\alpha} g^{\nu\beta} - g^{\mu\beta} g^{\nu\alpha}) F_{\mu\nu}}{(k^2 - M_W^2)^2}. \quad (45)$$

These effective propagators can be used and are useful when the particles in the loop are much bigger than the masses of the external particles. As an example we write down the loop integral for the diagram with soft photon emission from a t -quark, like the diagram in the middle of Fig. 5 (for $q = b$ and $\tilde{q} = t$):

$$T_{\mu\nu} = \int \int \frac{\bar{d}p \bar{d}r p_\mu r_\nu}{(p^2 - M_H^2)(p^2 - m_b^2)((r-p)^2 - M_W^2)(r^2 - M_W^2)(r^2 - m_t^2)^2}. \quad (46)$$

where $\bar{d}r \equiv d^d r / (2\pi)^d$ in d dimensions within dimensional regularization. A term with ultraviolet divergence appears if r_ν is replaced by p_ν in the numerator when doing loop integration in the subloop containing the integration over p . This happens for instance when the W -boson is replaced by an unphysical Higgs ϕ_\pm (the longitudinal W -components) within Feynman gauge, or if the left diagram in Fig. 6 is involved. Many loop diagrams are suppressed because of chirality ($P_L P_R = 0$), or asymmetric (odd) momentum integration like:

$$\int \bar{d}p f(p^2; \text{masses}) p^\mu = 0. \quad (47)$$

In the first subloop two Feynman parameters x and y are used. The result from the first subloop then depends on x and y and the squared loop momentum of the second loop.

Then the second loop integration is performed. In the end the Feynman parameter y is easily integrated out, and one is left with integration over the Feynman parameter x , to be done numerically.

The quantities S_i in (13) are dimensionless and given by integrals over one Feynman parameter. For the first diagram in Fig. 3 I find

$$S_1 = -u_t \int_0^1 dx \frac{[(1-3x) - \frac{u_t}{2}(1-x)]}{(u_t-1)(1-x)} \left\{ \ln \frac{C_1}{C_0} - \frac{u_H}{C_1 - u_H} \ln \left(\frac{C_1}{u_H} \right) + \frac{u_H}{C_0 - u_H} \ln \left(\frac{C_0}{u_H} \right) \right\}. \quad (48)$$

where the mass ratios u_t and u_H are given in (15). Terms suppressed by a factor of order m_b^2/m_t^2 with respect to the terms in (48) are neglected. Further,

$$C_0 \equiv C_0(x) = \frac{u_t}{x(1-x)}, \quad C_1 \equiv C_1(x) = \frac{1+x(u_t-1)}{x(1-x)}. \quad (49)$$

The term $\frac{u_t}{2}(1-x)$ in the numerator in (48) is due to the unphysical Higgs contribution which have to be added when the Feynman gauge for the W-propagator is used.

If the soft photon is emitted from the b -quark in the second diagram from left in Fig. 3 one obtains

$$S_2 = -\frac{u_t(1+\frac{u_t}{2})}{2(u_t-1)} \int_0^1 dx (1-2x) \left\{ -\text{dilog} \left(\frac{C_1}{u_H} \right) + \text{dilog} \left(\frac{C_0}{u_H} \right) \right\}, \quad (50)$$

where C_0 and C_1 are given as in (49) and the term proportional to $u_t \cdot u_t/2$ in the numerator is the unphysical Higgs contribution. The dilogarithmic function is in my case defined as

$$\text{dilog}(z) = \int_1^z dt \frac{\ln(t)}{(1-t)} = \text{Li}_2(1-z). \quad (51)$$

If the soft photon is emitted from the top quark after exchange of the Higgs boson, as in the third diagram from left in Fig. 3, or from soft photon emission from the W -boson in the fourth diagram, the left sub-loop containing the Higgs boson is logarithmically divergent. It turns out that for the third diagram in Fig. 3 the divergent part is projected out due to Dirac algebra (-technically, $\gamma_\alpha \sigma^{\mu\nu} \gamma^\alpha = 0$). One is then left with the finite part S_3^W :

$$S_3^W = \frac{u_t}{2(u_H-b)} \int_0^1 dx x [K(1, u_t; B_1) - K(1, u_t; B_0)] = 0.22, \quad (52)$$

where the function K is in general given by

$$K(A, a; B) \equiv -\frac{a}{(A-a)} \ln(B) + \frac{a^2}{(A-a)(B-a)} \ln\left(\frac{B}{a}\right) - \left(\frac{A}{A-a}\right)^2 \text{dilog}\left(\frac{B}{A}\right) + \left[\left(\frac{A}{A-a}\right)^2 - 1\right] \text{dilog}\left(\frac{B}{a}\right). \quad (53)$$

In eq. (52), one has :

$$B_0 = \frac{b + x(u_t - b)}{x(1 - x)} ; B_1 = \frac{u_H + x(u_t - u_H)}{x(1 - x)} , \quad (54)$$

where u_t and u_H are given in (15), and $b \equiv m_b^2/M_W^2$.

For the third diagram in Fig. 3, with W replaced by the unphysical Higgs ϕ_{\pm} the contribution is divergent, and given by

$$S_{3\Lambda}^{\phi} = u_t p_1(u_t) \cdot C_{\Lambda} = 3.42 C_{\Lambda} , \quad (55)$$

Divergent parts from the first subloop enters as

$$\ln(\Lambda^2/R) , \quad (56)$$

where R is a quantity depending on masses and Feynman parameters. The $\ln(R)$ term results in a finite term:

$$S_{3N}^{\phi} = -\frac{u_t^2}{(u_H - b)} \int_0^1 dx x(1 - x) [N(1, u_t; B_1) - N(1, u_t; B_0)] = -1.90 , \quad (57)$$

where $B_{0,1}$ are given in (54), and where in general:

$$\begin{aligned} N(C, A; B) \equiv & \frac{(A^2 - AB)}{C - A} \left(\frac{\ln(B)}{A} + \frac{\ln(\frac{B}{A})}{(B - A)} \right) \\ & + \frac{C(C - B)}{(C - A)^2} \left\{ \frac{1}{2} [\ln(B - C)]^2 + \text{dilog}\left(\frac{B}{B - C}\right) - \ln(C) \cdot \ln(B - C) \right\} \\ & + \frac{[BC - A(2C - A)]}{(C - A)^2} \left\{ \frac{1}{2} [\ln(B - A)]^2 + \text{dilog}\left(\frac{B}{B - A}\right) - \ln(A) \cdot \ln(B - A) \right\} . \end{aligned} \quad (58)$$

Further, there is a non-logarithmic finite term (not in $\ln(R)$ in eq. (56)):

$$S_{3K}^{\phi} = \frac{u_t^2}{2(u_H - b)} \int_0^1 dx x(2x - 3) [K(1, u_t; B_1) - K(1, u_t; B_0)] = 3.49 \quad (59)$$

where $B_{0,1}$ are given in (54), and K is given in (53). The total S_3 :

$$S_3 = S_3^W + S_{3\Lambda}^{\phi} + S_{3N}^{\phi} + S_{3K}^{\phi} , \quad (60)$$

is then given in (18).

For the fourth (divergent) diagram with soft photon emission from the W -boson, I find

$$S_{4\Lambda} = -\frac{3}{4} p_2(u_t) C_{\Lambda} = -0.91 C_{\Lambda} . \quad (61)$$

The logarithmic ($\sim \ln(R)$) type finite term from (56) is

$$S_{4N} = \frac{3u_t}{2(u_H - b)} \int_0^1 dx x(1-x)[N(u_t, 1; B_1) - N(u_t, 1; B_0)] = 2.12, \quad (62)$$

where $B_{0,1}$ are still given in (54). For the non-logarithmic finite term

$$S_{4K} = -\frac{3u_t}{2(u_H - b)} \int_0^1 dx x(x-2) [K(u_t, 1; B_1) - K(u_t, 1; B_0)] = 0.86, \quad (63)$$

where the function K is given in (53), and where $B_{1,0}$ are given as in (54). The total S_4 :

$$S_4 = S_{4\Lambda}^\phi + S_{4N}^\phi + S_{4K}^\phi \quad (64)$$

is given in (21). Note that S_3^ϕ is of the order m_t^4 in contrast to $S_{1,2}$, S_3^W and S_4 which are of the order m_t^2 .

The mathematical expression for the loop functions $f(q, \tilde{q})$ in (26)-(32) for soft photon emission from the quark q given in the left of Figure 5 is given by

$$f(q, \tilde{q}) = \frac{1}{1-b} \int_0^1 dx [K(u_H, a; D_1) - K(u_H, a; D_0)] \left\{ x - \frac{b}{4}(1-2x) \right\}, \quad (65)$$

where u_H is given in (15) and

$$a \equiv \frac{(m_q)^2}{M_W^2}, \quad b \equiv \frac{(m_{\tilde{q}})^2}{M_W^2}. \quad (66)$$

Further,

$$D_0 \equiv D_0(x) \equiv \frac{b+x(1-b)}{x(1-x)} \quad D_1 \equiv D_1(x) \equiv \frac{1}{x(1-x)}. \quad (67)$$

In the $f(q, \tilde{q})$'s in eq. (65) the unphysical Higgs (ϕ_\pm) contribution (proportional to $-b/4$) within Feynman gauge for the W -boson are also included. The numbers are given in tables I and II below. The f -functions are not directly proportional to quark masses as for the S_i functions in section III. Therefore the individual terms are calculated separately before performing the GIM-cancellation, namely, to obtain $f(b, t-c)$, both $f(b, t)$ and $f(b, c)$ are needed. The same is the case for $h(b, t-c)$ and $k(b, t-c)$ below. This is in contrast to the amplitudes in section III, where diagrams involving the c -quark can be safely neglected.

For emission from the quark \tilde{q} in the diagram in the middle of Fig. 5, we obtain the loop functions $h(q, \tilde{q})$ in (68), which is similar to (65) but with M_H replaced by M_W and $m_q \leftrightarrow m_{\tilde{q}}$ i.e $u_H \rightarrow 1$ and $a \leftrightarrow b$. I have split the functions h in a logarithmic divergent

quark \tilde{q}	$f(s, \tilde{q})$	$f(b, \tilde{q})$
u	0.296731	0.293166
c	0.296656	0.293092
t	-0.047004	-0.047305

TABLE I: Values for the loop function $f(q, \tilde{q})$ for EDM of the d quark.

quark \tilde{q}	$f(c, \tilde{q})$	$f(t, \tilde{q})$
d	0.2962815	1.136204
s	0.2962810	1.136201
b	0.2954856	1.131829

TABLE II: Values for the loop functions $f(q, \tilde{q})$ for EDM of the u quark.

part h_Λ , the associated finite logarithmic part h_N coming from $\ln(R)$ in (56) due to the unphysical Higgs (see eq. (69), and the non-logarithmic finite part h_K (see eq. (71)):

$$h = h_\Lambda + h_N + h_K \quad (68)$$

The logarithmic term $h_N(q, \tilde{q})$ in (68) is given by

$$h_N(q, \tilde{q}) = -\frac{b}{(u_H - a)} \int_0^1 dx x(1-x) [N(1, b; B_1) - N(1, b; B_0)] , \quad (69)$$

where u_H is given in (15), and a, b in (66), and

$$B_1 = \frac{u_H + x(1 - u_H)}{x(1 - x)}; \quad B_0 = \frac{a + x(1 - a)}{x(1 - x)} . \quad (70)$$

The finite non-logarithmic part h_K is given by

$$h_K(q, \tilde{q}) = \frac{1}{u_H - a} \int_0^1 dx x \left(1 - \frac{b}{2}(1 + x)\right) [K(1, b; B_1) - K(1, b; B_0)] . \quad (71)$$

The term proportional to $b/2$ above is the finite part of the unphysical Higgs contribution. The functions h_K are given in tables III and IV.

Numerically, we find for the three numerically relevant quantities in $\Delta h_d(b, t - c)$:

$$\Delta h_{d\Lambda} = p_2(u) \cdot C_\Lambda \simeq 1.22 C_\Lambda , \quad \Delta h_{dN} = 0.39 , \quad \Delta h_{dK} = -1.65 . \quad (72)$$

For other cases the Δh 's are of order 10^{-3} or smaller. Similar to the case with emission from quark q , the contribution involving the top quark proportional to ξ_t gives the biggest contributions after GIM-cancellation, as in the preceding section.

quark \tilde{q}	$h_K(s, \tilde{q})$	$h_K(b, \tilde{q})$
u	0.348206	0.347882
c	0.347396	0.347073
t	-1.300107	-1.298341

TABLE III: Values for the loop function h_K for EDM of the d quark

quark \tilde{q}	$h_K(c, \tilde{q})$	$h_K(t, \tilde{q})$
d	0.3481758	0.2108653
s	0.3481687	0.2108620
b	0.3417355	0.2077501

TABLE IV: Values for the loop function h_K for EDM of the u quark

Now, the next step is to calculate the loop diagrams when the soft photon is emitted from a W -boson. Again, I have split the functions k in a non-logarithmic finite part k_K , the divergent part k_Λ due to unphysical Higgs, and the finite logarithmic part k_N (associated with $\ln(R)$ -terms):

$$k = k_\Lambda + k_N + k_K . \quad (73)$$

For the diagram to the right in Fig. 5 the loop function is

$$k(q, \tilde{q})_1 = \frac{1}{(u_H - a)} \int_0^1 dx x [K(b, 1; B_1) - K(b, 1; B_0)] . \quad (74)$$

where $B_{0,1}$ are given as in (70), and a and b are given in (66).

When the soft photon is emitted instead from the W -boson in the middle of diagram one obtains

$$k(q, \tilde{q})_2 = \frac{1}{(u_H - a)} \int_0^1 \frac{dx x}{1-x} [K_{W2}(B_1) - K_{W2}(B_0)] , \quad (75)$$

where the function $K_{W2}(B)$ is given by

$$K_{W2}(B) = \frac{B^2 \ln(B)}{(B-1)(B-b)} . \quad (76)$$

with $B_{0,1}$ still given as in (70).

For the diagram to the right of Fig. 5 with the W in the middle replaced by an unphysical Higgs ϕ_\pm , one obtains

$$k_3 = (k_\Lambda + k_N) + \frac{b}{4} k_1 + \tilde{k}_3 , \quad (77)$$

where k_Λ is the divergent part shown in (86), and the logarithmic finite part is

$$k_N(q, \tilde{q}) = -\frac{b}{2(u_H - a)} \int_0^1 dx x(1-x) (N(1, b; B_1) - N(1, b; B_0)) , \quad (78)$$

and

$$\tilde{k}(q, \tilde{q})_3 = \frac{-b}{4(u_H - a)} \int_0^1 dx x^2 [K(b, 1; B_1) - K(b, 1; B_0)] , \quad (79)$$

where $B_{0,1}$ are given as in (70).

With emission from the W in the middle and when the W to the right is replaced by an unphysical Higgs one obtains

$$k(q, \tilde{q})_4 = -\frac{b}{4} k(q, \tilde{q})_2 + \tilde{k}(q, \tilde{q})_4 , \quad (80)$$

with

$$\tilde{k}(q, \tilde{q})_4 = \frac{-b}{4(u_H - a)} \int_0^1 dx x [K_{W4}(B_1) - K_{W4}(B_0)] , \quad (81)$$

where

$$K_{W4}(B) = \Delta K_{W4}(B) + \frac{x}{(1-x)} K_{W2}(B) , \quad (82)$$

where $K_{W2}(B)$ is given previously in eq (76), and where

$$\Delta K_{W4}(B) = \frac{2}{(1-b)} \left(b \cdot \text{dilog}\left(\frac{B}{b}\right) - \text{dilog}(B) \right) , \quad (83)$$

The total finite amplitude for emission from W 's (k_Λ and k_N excluded) is

$$k_K = k_1(1 + b/4) + k_2(1 - b/4) + \tilde{k}_3 + \tilde{k}_4 , \quad (84)$$

and the numerical values for the amplitudes k_K are given in tables V and VI. In eqs. (74) and (75) the terms proportional to $b/4$ are due to the unphysical Higgs contribution in Feynman gauge.

quark \tilde{q}	$k(s, \tilde{q})_K$	$k(b, \tilde{q})_K$
u	0.862602	0.862201
c	0.861867	0.861466
t	-1.229824	-1.234307

TABLE V: Values for the loop function k_F for EDM of the d quark

quark \tilde{q}	$k(c, \tilde{q})_K$	$k(t, \tilde{q})_K$
d	0.862565	0.585069
s	0.862561	0.585067
b	0.858181	0.582868

TABLE VI: Values for the loop function k_F for EDM of the u quark

For diagrams with a soft photon emitted from some W -boson in Fig. 5, the numerically relevant part is

$$\left(\frac{d_d}{e}\right)_W \simeq 3 \hat{e}_W F_2 \text{Im} [Y_R(d \rightarrow b) \xi_t] \cdot \Delta k_d(b, t - c), \quad (85)$$

Numerically, we find for the parts of $\Delta k_d(b, t - c)$:

$$\Delta k_{d\Lambda} = \frac{1}{2} p_2(u) \cdot C_\Lambda \simeq 0.61 C_\Lambda ; \quad \Delta k_{dN} = -0.38 , \quad \Delta k_{dF} = -2.10 , \quad (86)$$

Other Δk 's are of order 10^{-3} or smaller.

Acknowledgments

I am grateful to Svjetlana Fajfer for suggesting these calculations and for valuable discussions. Useful comments by Lluís Oliver and Ivica Picek are also acknowledged.

I am supported in part by the Norwegian research council (via the HEPP project).

-
- [1] M. Pospelov and A. Ritz, *Annals Phys.* **318** (2005) 119 [hep-ph/0504231]
 - [2] T. Fukuyama, *Int. J. Mod. Phys.* **A27** (2012) 1230015, arXiv: 1201.4252 [hep-ph]
 - [3] W. Dekens, J. de Vries, J. Bsaisou, W. Bernreuther, C. Hanhart, Ulf-G. Meiner, A. Nogga, and A. Wirzba *JHEP* **07** (2014) 069, arXiv:1404.6082[hep-ph]
 - [4] M. Jung and A. Pich, *JHEP* **1404** 076, arXiv:1308.6283 [hep-ph]
 - [5] N. Yamanaka, B.K. Sahoo, N. Yoshinaga, T. Sato, K. Asahi, and B. P Das, *Eur. Phys. J.*, **A53** (2017) 54, arXiv: 1703.01570 [hep-ph]
 - [6] K. A. Olive et al [Particle Data Group Collaboration] : “*Review of Particle Physics*”, *Chin. Phys.* **C40** (2016) 100001

- [7] C. A. Baker, D. D. Doyle, P. Geltenbort, K. Green, M. G. D. van der Grinten, P. G. Harris, P. Iaydjiev and S. N. Ivanov *et al.*, *Phys. Rev. Lett.* **97** (2006) 131801 [hep-ex/0602020].
- [8] E.P. Shabalina, E.P., *Yad.Fiz.* **31** (1980)1665-1679 (*Sov. J. Nucl.Phys.* **31** (1980) 864)
- [9] A. Czarnecki, and B. Krause, *Phys.Rev.Lett.* **78** (1997) 4339 [hep-ph/97043559]
- [10] A. Maiezza, and M. Nemevšek, *Phys. Rev. D* **90** (2014) 095002, arXiv:1407.3678 [hep-ph]
- [11] D.V. Nanopoulos, A. Yildiz, and P. H. Cox, *Phys.Lett.* **B87** 53
- [12] B.F. Morel, *Nucl.Phys.* **B157** (1979) 23
- [13] M.B. Gavela, A. Le Yaouanc, L. Oliver, O. Pene J.C. Raynal, and T.N. Pham, *Phys.Lett.* **B109** (1982) 215
- [14] I.B. Khriplovich and A.R. Zhitnitsky, *Phys.Lett.* **B109** (1982) 490
- [15] B.H.J. McKellar, S.R. Choudhury, X.-G. He and S. Pakvasa, *Phys.Lett.* **B197** (1987) 556
- [16] J.O. Eeg, J.O. and I. Picek, *Phys.Lett.* **B130** (1983) 308
- [17] J.O. Eeg, and I. Picek, *Nucl.Phys.* **B244** (1984) 77
- [18] C. Hamzaoui and A. Barroso, *Phys. Lett. B* **154**, 202 (1985).
- [19] T. Mannel and N. Uraltsev, *Phys. Rev. D* **85** (2012) 096002, arXiv:1202.6270 [hep-ph]
- [20] T. Bhattacharya, V. Cirigliano, R. Gupta, H-W. Lin, and B. Yoon, *Phys. Rev. Lett.* **115** (2015) 212002, arXiv:1506.04196 [hep-lat]
- [21] T. Bhattacharya, V. Cirigliano, S. D. Cohen, R. Gupta, A. Joseph, H-W. Lin, and B. Yoon, *Phys. Rev. D* **92** (2015)094511 , arXiv:1506.06411 [hep-lat]
- [22] W. Buchmuller and D. Wyler, *Phys.Lett.* **B121** (1983) 321
- [23] W. Altmannshofer, A. J. Buras and P. Paradisi, *Phys. Lett. B* **688** (2010) 202 [arXiv:1001.3835 [hep-ph]].
- [24] A. J. Buras, G. Isidori and P. Paradisi, *Phys. Lett. B* **694** (2011) 402, arXiv:1007.5291 [hep-ph]
- [25] J. Brod, U. Haisch, and J. Zupan, *JHEP* **1311** (2013) 180, arXiv:1310.1385 [hep-ph]
- [26] A. V. Manohar and M. B. Wise, *Phys. Rev. D* **74** (2006) 035009 [hep-ph/0606172].
- [27] G. Degrossi and P. Slavich, *Phys. Rev. D* **81** (2010) 075001, arXiv:1002.1071 [hep-ph]
- [28] Xiao-Gang He, Chao-Jung Lee, Siao-Fong Li, and J. Tandean, arXiv:1404.4436 [hep-ph]
- [29] J. M. Arnold, B. Fornal and M. B. Wise, *Phys. Rev. D* **87** (2013) 075004, arXiv:1212.4556 [hep-ph]
- [30] K. Fuyuto, J. Hisano, and E. Senaha, arXiv:1510.04485 [hep-ph]
- [31] L. Bian, and N. Chen, arXiv: 1608.07975 [hep-ph]

- [32] S. Fajfer, and J.O. Eeg, *Phys. Rev.* **D89** (2014) 095030, arXiv:1401.2275 [hep-ph]
- [33] W. Altmannshofer, R. Primulando, C. -T. Yu and F. Yu, *JHEP* **1204** (2012) 049, arXiv:1202.2866 [hep-ph]
- [34] A. Goudelis, O. Lebedev, and J-h. Park, *Phys. Lett.* **B707** (2012) 369-374, arXiv:1111.1715 [hep-ph]
- [35] G. Blankenburg, J. Ellis, and G. Isidori, *Phys. Lett.* **B712** (2012) 386-390; arXiv:1202.5704 [hep-ph]
- [36] R. Harnik, J. Kopp and J. Zupan *JHEP* **03** (2013) 036, arXiv:1209.1397 [hep-ph]
- [37] A. Greljo, and J.F. Kamenik, and J. Kopp, *JHEP* **07** (2014) 046 arXiv 1404.1278 [hep-ph]
- [38] M. Gorbahn, and U. Haisch, *JHEP* **06** (2014) 033, arXiv 1404.4873 [hep-ph]
- [39] I. Doršner, S. Fajfer, A. Greljo, J. Kamenik, Jernej F. , N. Košnik, and I. Nišandžic, *JHEP* **06** (2015) 108, arXiv 1502.07784 [hep-ph]
- [40] S.M. Barr and A. Zee, *Phys. Rev. Lett.* **65** (1990) 21-24 [Erratum: *Phys. Rev. Lett.* **65** (1990) 2920]
- [41] D.Chang, W.S. Hou, and W.-Y. Keung,, *Phys. Rev.***D48** (1993) 217; hep-ph/9302267
- [42] R.G. Leigh, R. G., S. Paban, S. and R. M. Xu, *Nucl. Phys.* **B352** (1991) 45-58
- [43] J.D. Bjorken, and S. Weinberg, *Phys. Rev. Lett.* **38** (1977) 622
- [44] G.F. Giudice, and O. Lebedev, *Phys. Lett.* **B665** (2008) 79-85, arXiv: 0804.1753 [hep-ph]
- [45] W. Altmannshofer, J. Brod, and M. Schmaltz, *JHEP* **05** (2015) 125, arXiv 1503.04830 [hep-ph]
- [46] L.J Reinders, H. Rubinstein, and S. Yazaki, *Phys.Rept.* **127** (1985) 1